Chapter 3

In situ development of bio-based polyurethane-blended-epoxy hybrid materials and its nanocomposites with modified graphene oxide via non-isocyanate route

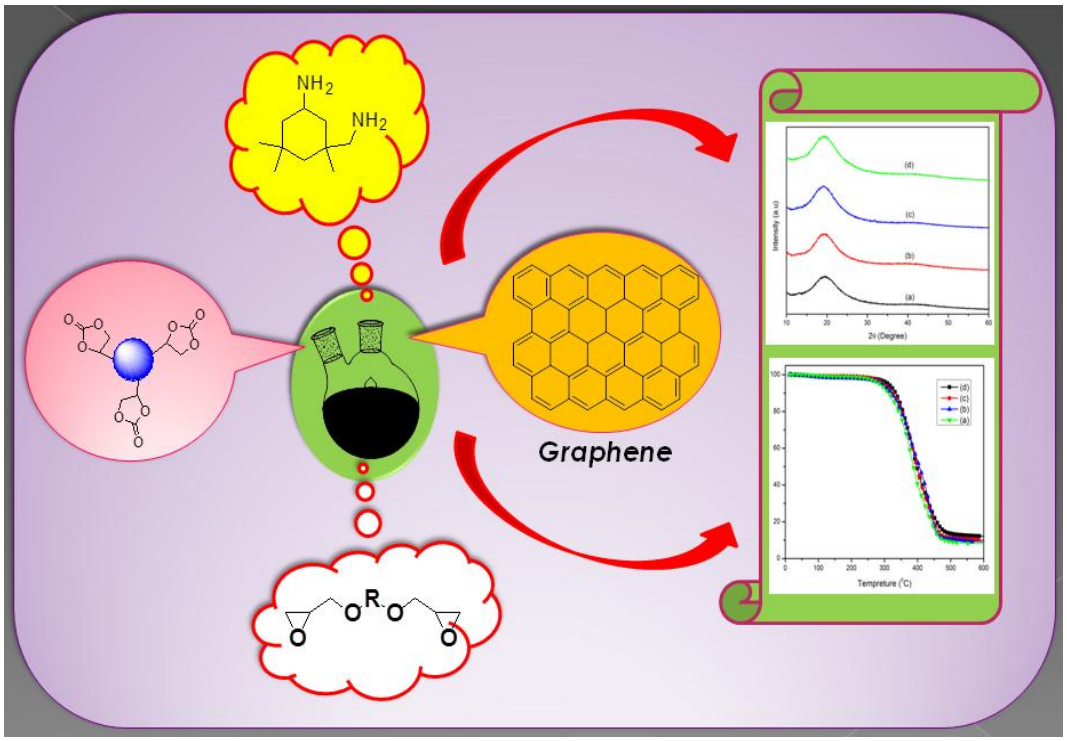

Sunflower oil based hybrid non-isocyanate polyurethane and its nanocomposites are synthesized by blending of carbonated sunflower oil with epoxy resin and incorporating graphene oxide to get improved mechanical and thermal properties

3.1 Introduction:

Polyurethane (PU) is the sixth most broadly used polymer with numerous applications [1]. PUs is multipurpose polymeric materials with extensive demand due to their special properties like superior tensile strength, high flexibility and solvent resistance [2–7]. Usually, PU is obtained by treating a polyol with a polyisocyanate, which are based on fossil resources. The isocyanates are highly noxious and volatile materials prepared from phosgenation of diamines, and long-time exposure causes several damaging health effects [1]. For that reason, a non-isocyanate (the so-called NIPU: non-isocyanate polyurethane) synthetic way needs to be developed for replacing isocyanates in the production of PU from renewable resources. The most investigated isocyanate-free methods include transurethane polycondensation of various amines and alcohols [8], AB type self condensation [9] and aminolysis of cyclic carbonate [10]. However, among these routes, the most attractive one is the step-growth polyaddition of diamines with dicyclocarbonates that leads to NIPU production. This cyclic carbonate is obtained by the reaction of epoxy group containing compounds with carbon dioxide (CO_2). CO_2 is one of the major greenhouse gases that is the reason of global warming, weather alteration and the major climatic concerns in the 21st century [11]. Therefore, from the perspective of environmental safety and resource consumption, the use of CO_2 into valuable chemicals and materials is an essential issue. In the meantime, it is also an inexpensive, recyclable, abundant and non-toxic resource [12,13]. In this approach, each repeating unit of the resulting NIPUs contains a hydroxyl group after the polymerization that thermal stability of the NIPU in comparison that of conventional PU [10,14–16].

This part of the thesis is published in

Doley, S., Sarmah, A., Sarkar, C., and Dolui, S. K. *In situ* development of bio-based polyurethane-*blend*-epoxy hybrid materials and their nanocomposites with modified graphene oxide via non-isocyanate route. *Polymer International*, 67(8):1062-1069, 2018.

NIPUs are regularly synthesized from petro-based molecules and recently various vegetable oils [16–18] are being gradually used as renewable resources for the synthesis of it [19–21]. The synthesis of polymers from vegetable oils has attained tremendous interest in the recent years because of their economical, worldwide availability and the shrinking of petroleum resources [22].

However, in contrast to the conventional PUs, NIPUs possess low molecular weight and mechanical properties because of the side reactions and low reactivity between cyclic carbonate and primary amine or amide [23–25]. Therefore, to enhance the properties of NIPU, it is desirable to develop different catalysts to improve the reactivity of amines towards the cyclic carbonate, and also to design molecular structures having upto six- or seven-membered reactive cyclic carbonates [26–29]. To enhance the physical properties of NIPUs, researchers have started developing hybrid NIPU (HNIPU), wherein NIPU is crosslinked with other appropriate resins like amino resin, epoxy resin, ketonic resin and silicone resin [29–31].

In this study, we have developed bio-based HNIPU by using renewable sunflower oil as the raw material and commercial epoxy resin as the chain extender. However, the overall outcome of vegetable oil based HNIPUs are still away from satisfactory. In this respect, nanotechnology plays a major role. Recently, the nanocomposites of polymer with carbon based nanomaterials have obtained considerable attention due to the incorporation of such nanomaterials can efficiently increase the properties of the pristine polymer such as mechanical, thermal and electrical properties [32–34]. Among the various types of carbon based nanomaterials, graphene, a single-atom-thick sheet has been broadly considered because of its exceptional properties such as high aspect ratio, outstanding chemical, thermal stability and chemical inertness etc [35,36]. Furthermore, the chemical functionalization on the graphene oxide (GO) surface can be used to improve its interactions with the polymer matrix. This can result in better compatibility between the GO and polymer network and thus improve the properties of the composite materials [33].

Motivated from the above discussion, to further improve the physicochemical properties of HNIPU, amine functionalized graphene oxide (AF-GO) is incorporated into

the polymer network of HNIPU and the effect of different wt% of AF-GOs on the properties of the HNIPU is examined.

3.2. Experimental

3.2.1 Materials

Graphite flakes were purchased from Sigma Aldrich with a particle size of 150 μm and purity of 99.9%. (3-aminopropyl)trimethoxysilane (APTMS, Assay 97%) were also purchased from Sigma Aldrich, India. Epoxy resin (epoxy equivalent: 170-180 g per eq) was obtained from Kumud Enterprise, Kharagpur, West Bengal, India. All the other chemicals used for the experiments are the same as explained in section 2.2.1 of Chapter 2.

3.2.2 Preparation of carbonated sunflower oil (CSFO)

Sunflower oil based cyclic carbonates were prepared by reaction of CO_2 with epoxidized sunflower oil (ESFO) at 120 °C and 50 bar CO_2 pressure for 10 h in a reactor catalyzed by tetra-n-butylammonium bromide (TBABr) (3.5 mol% with respect to ESFO). Once the reactor cooled down and the gas discharged by venting, the final viscous product was collected.

3.2.3 Amine modification of graphene oxide (AF-GO)

The synthesis process of amine-functionalized graphene oxide (AF-GO) is as follows: in the first step, graphene oxide was prepared from natural graphite powder by following the modified Hummer's procedure. In the second step, 25 mg GO was dispersed by sonication in distilled water for 1 h and then 5 mL toluene solution containing (3-aminopropyl)trimethoxysilane (APTMS) was subsequently added into the above solution. Then, the mixture was refluxed at 90 ºC for 24 h. The product amine-functionalized graphene oxide (AF-GO) was filtered, and subsequently washed with distilled water and acetone and kept at 60 ºC for 24 h **(Scheme 3.1)** [37].

3.2.4 Preparation of hybrid HNIPUs

Hybrid HNIPUs were prepared by the reaction of isophorone diamine (IPDA) with a mixture of CSFO and different wt% of epoxy resin (10, 20, and 30% with respect

to CSFO) at 70 °C for 3-4 h in tetrahydrofuran (THF). For all the samples, the ratio of amine equivalents to the epoxy and CSFO equivalents was taken at 1:1 equivalent. The final product was placed onto a Teflon sheet and kept at 90 °C for 48 h and then heated to 130 °C for 1 h to achieve fully cured film. The obtained polymer with 10, 20, and 30 wt% are encoded as HNIPU10, HNIPU20 and HNIPU30 respectively.

3.2.5 Preparation of HNIPU/AF-GO nanocomposite

The nanocomposites of the hybrid HNIPU30 were prepared by incorporating (amine-functionalized graphene oxide) AF-GO at 0.3, 0.6 and 1.0 wt% **(Table 3.1)**. Firstly, AF-GO was dispersed in tetrahydrofuran (THF) by sonication for 1 h to obtain a dispersed suspension. After obtaining a uniform dispersion of AF-GO in THF, it was poured into the mixture of CSFO and epoxy resin with continuous stirring at 85 °C for 3-4 h with the addition of isophorone diamine (IPDA) as the curing agent. The resulting mixture was then kept on a Teflon sheet and cured similarly as the above procedure.

Table 3.1: Composition of the nanocomposites.

Sample name	CSFO (g)	Epoxy resin (wt%)	AF-GO (wt%)
HNC0.3	100	30	0.3
HNC0.6	100	30	0.6
HNC1.0	100	30	1.0

**HNC0.3 stands for the hybrid nanocomposites with 0.3 wt% of AF-GO and so on.*

3.2.6 Characterizations

The X-ray diffraction (XRD) diffractograms of the polymer matrix were measured by using a P-XRD diffractometer (Model: D8 FOCUS, Bruker AXS, Germany) operating at a wavelength of 1.5 Å. To observe the dispersion, intercalation and exploitation of AF-GO sheets, a transmission electron microscope (JEOL, JEM 2100) was used. The instruments used for characterization including FT-IR, SEM, TGA, UTM and scratch hardness tester are mentioned in section 2.2.4 of Chapter 2. Small part of the cured films was kept in different concentration solutions to examine the chemical resistance of prepared films.

3.3 Results and discussion

3.3.1 FT-IR analysis

3.3.1.1 Amine functionalization of GO

FT-IR spectra of GO and AF-GO are presented in **Fig. 3.1**. In the FT-IR spectrum of GO (**Fig. 3.1a**), the peak appears at 1732 and 1391 cm^{-1} related to the C=O stretching vibrations of the COOH groups and the broad peak at 3421 cm^{-1} is due to OH vibrations. The peaks 1623, 1215 and 1059 cm^{-1} are corresponding to the C=C skeletal vibration and C-O stretching respectively [37]. The peaks in the range of 2853-2922 cm^{-1} are observed in both GO and AF-GO spectra due to C-H stretching. The results signify that the COOH and OH groups were successfully introduced at the surface of the graphite. In the spectra of AF-GO (**Fig. 3.1b**), the disappearance of the peaks located at 1723 and 1391 cm^{-1}, and the new peaks at 1092 and 693 cm^{-1} are due to Si-O-C bands. The signal at 757 cm^{-1} is due to the overlap of Si-H and NH_2 vibration bands suggesting that the GO has reacted with APTMS. Further, the characteristic peaks at 1580, 1223 and 3409 cm^{-1} are attributed to primary amine groups, C-N and N-H stretching vibrations respectively [32]. The whole reaction process is represented diagrammatically in **Scheme 3.1**.

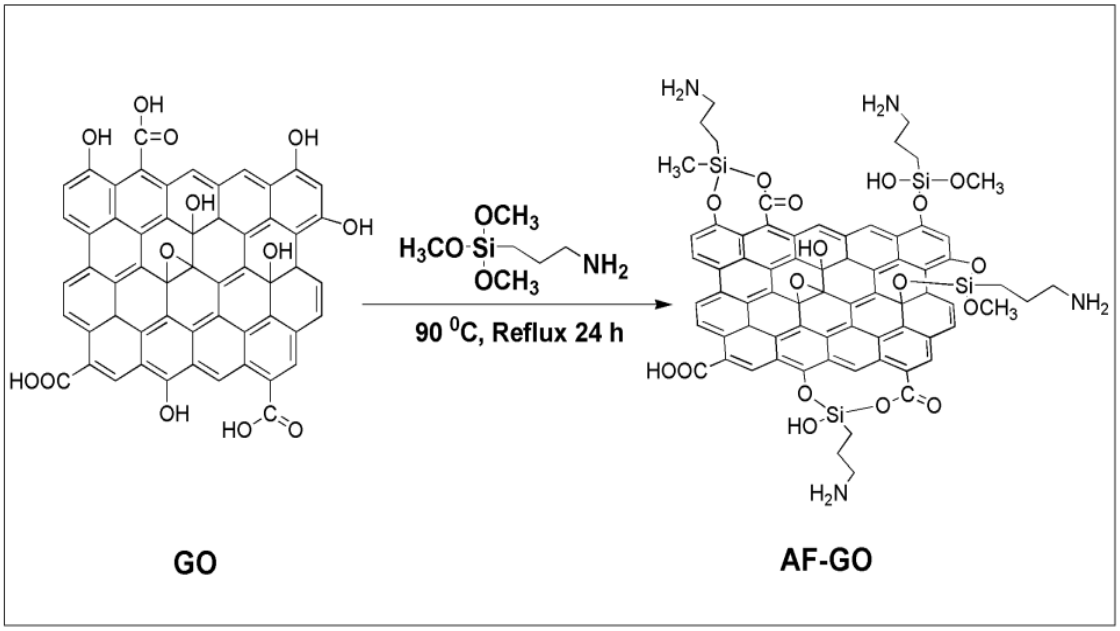

Scheme 3.1: Amine functionalization of GO.

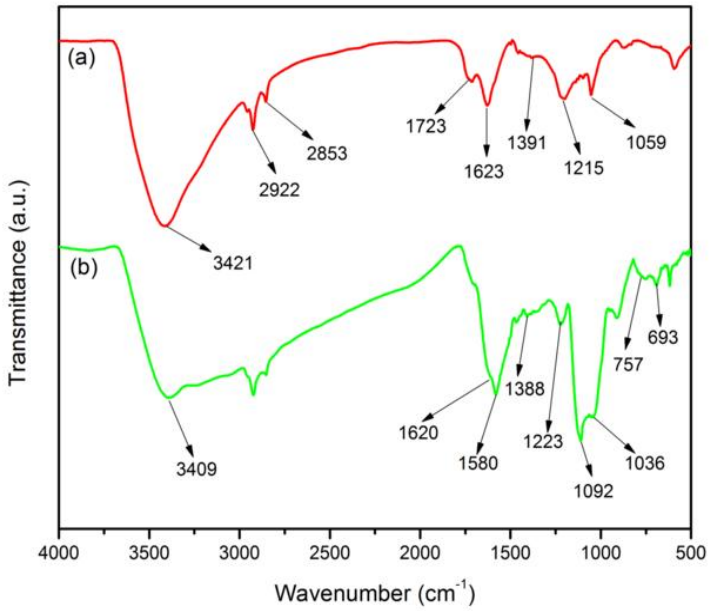

Fig. 3.1: FT-IR spectra of (a) GO and (b) AF-GO.

3.3.1.2 Preparation of HNIPU/AF-GO nanocomposite

FT-IR spectra of (a) epoxy resin (b) CSFO, (c) CNT0 and (d) HNC1.0 are presented in **Fig. 3.2**. In the FT-IR spectra of epoxy resin (**Fig. 3.2a**), the peaks at 931,

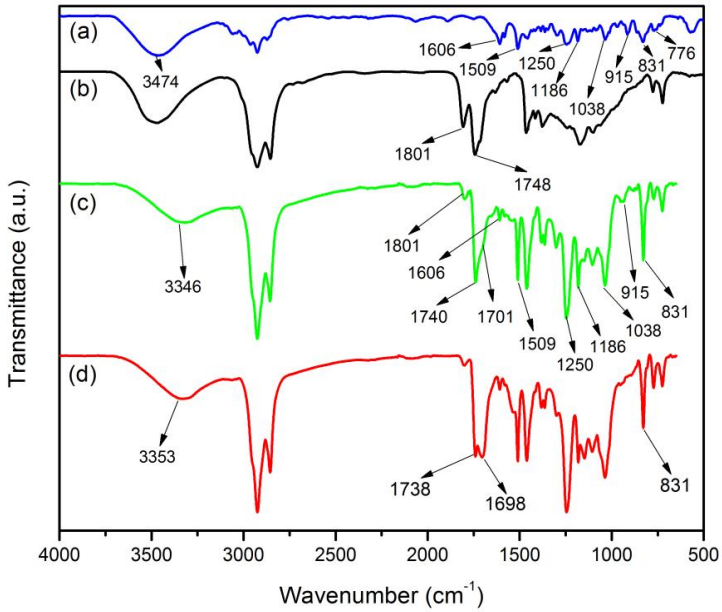

Fig. 3.2: FT-IR spectra of (a) epoxy resin (b) CSFO and ATR-FT-IR (c) HNIPU30 and (d) HNC1.0.

830 and 1186 cm^{-1} correspond to the stretching of C-O, C-O-C of epoxy group and aromatic C-O stretching respectively, and the signal about 3474 cm^{-1} is due to the presence of OH groups of epoxy resin. The peaks appearing at 1509-1606, 1250 and 1035 cm^{-1} are related to the aromatic C=C bonds, phenolic C–O groups, and stretching of C-O-C of ether respectively [38]. In the FT-IR spectra of CSFO (**Fig. 3.2b**), the peak for C=O stretching vibration of triglyceride appears at1748 cm^{-1} and the peak for 1801 cm^{-1} is assigned to C=O of cyclic carbonate.

FT-IR spectral data of HNIPU30 and HNC1.0 indicate the presence of important linkages such as ester groups, aromatic C=C bonds, phenols C-O, ether linkages etc. The broad peak at 3346-3353 cm^{-1} is because of the OH groups generated in the polymerization reaction as well as -NH stretching. In FT-IR spectrum of HNIPU30 (**Fig. 3.2c**), the appearance of a shoulder peak on ester of the oil at 1701 cm^{-1} indicates the formation of urethane along with a significant amount of residual cyclic carbonate at 1801 cm^{-1} and epoxy peak at 931 cm^{-1}. Since the amine groups are reactive towards both epoxy and cyclic carbonates, after the addition of amine-functionalized AF-GO it can react with both epoxy and carbonate groups and can be formed bonds between the HNIPU30 and AF-GO. **Fig. 3.2d** shows the negligible effect of the AF-GO on the spectra of HNC1.0, indicating that it is difficult to directly identify the formation of urethane bonds between the HNPU30 and AF-GO because HNPU30 backbones have the same chemical bonds with HNC1.0. In addition, the peak at 831 cm^{-1} due to the peak overlapping with in plane flexural vibration of CH_3 groups [29].

3.3.2 XRD analysis

XRD studies were performed to observe whether there is a change in the structure of GO, AF-GO and nanocomposites. **Fig. 3.3** shows XRD patterns for GO and AF-GO. For GO, the peak at $2\theta = 10.71°$ corresponds to the (001) plane having an interlayer spacing of 0.82 nm, which indicates a highly ordered structure. This large interlayer spacing is due to the generation of oxygen-containing functional groups after oxidization. This peak is sharp due to the agglomeration and accumulation of GO via the formation of hydrogen bond among the nanosheets [39].

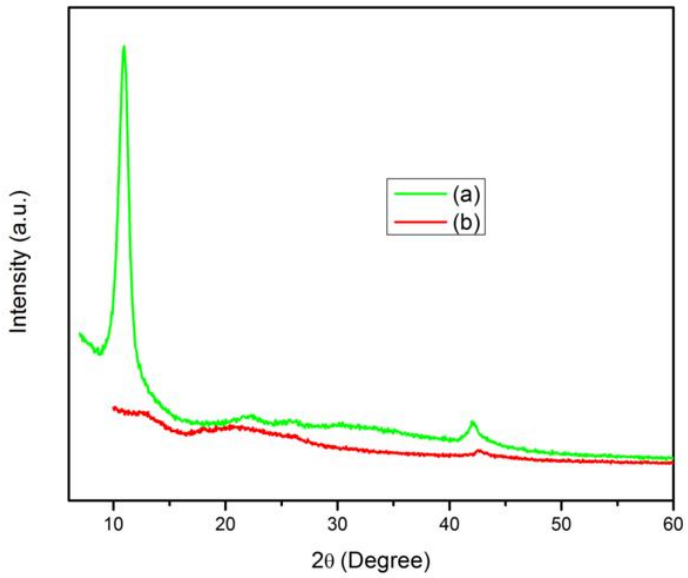

Fig. 3.3: XRD patterns of (a) GO and (b) AF-GO.

The peak at 2θ = 42.16° indicates the long range order of graphite. After the chemical treatment of GO with APTMS, due to covalent fixation of silane groups in the GO layers, the distinctive peaks of GO disappear. This results in the full exfoliation of GO and prohibits its aggregation [36,37]. It suggests that the APTMS chains are successfully incorporated on the surface of GO sheets to exfoliate them, which agrees well with the FT-IR result **(Fig. 3.1b)**.

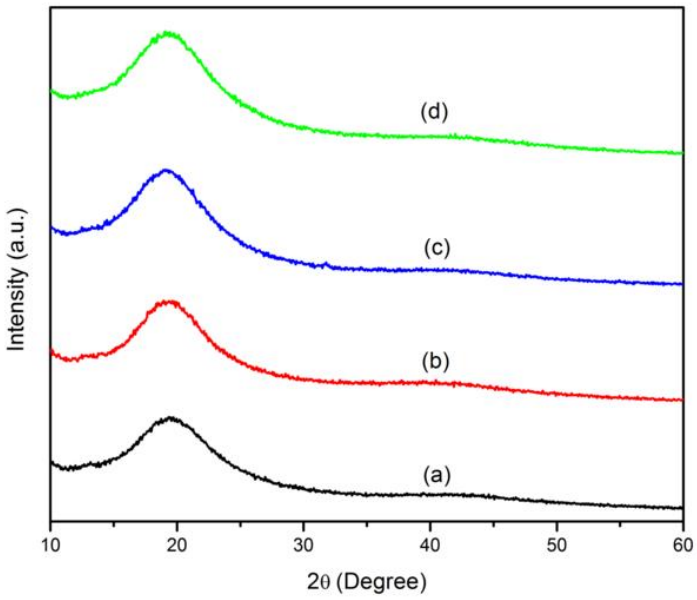

Fig. 3.4: XRD patterns of (a) HNIPU30, (b) HNC0.3 (c) HNC0.6 and (d) HNC1.0.

XRD pattern of the nanocomposites is displayed in **Fig. 3.4**. XRD pattern of the pristine blend (HNIPU30) and the nanocomposites shows a broad diffraction peak at around 2θ = 19.01° which reveals its amorphous nature. Thus, XRD studies suggest the formation of fully exfoliated and homogeneous distribution of AF-GO within the polymer matrix.

3.3.3 Morphological analysis

The interfacial adhesion between AF-GO and the polymer matrix was further studied using SEM imaging and are shown in **Fig. 3.5**. The surface of the HNIPU30 resin is represented in **Fig. 3.5a** which shows a smooth surface with river-like patterns. The incorporation of AF-GO into the polymer matrix exhibits a rough surface morphology with many sheet-like features **(Fig. 3.5b)**. This indicates the reinforcement of AF-GO in the HNIPU matrix (**Scheme 3.2)**.

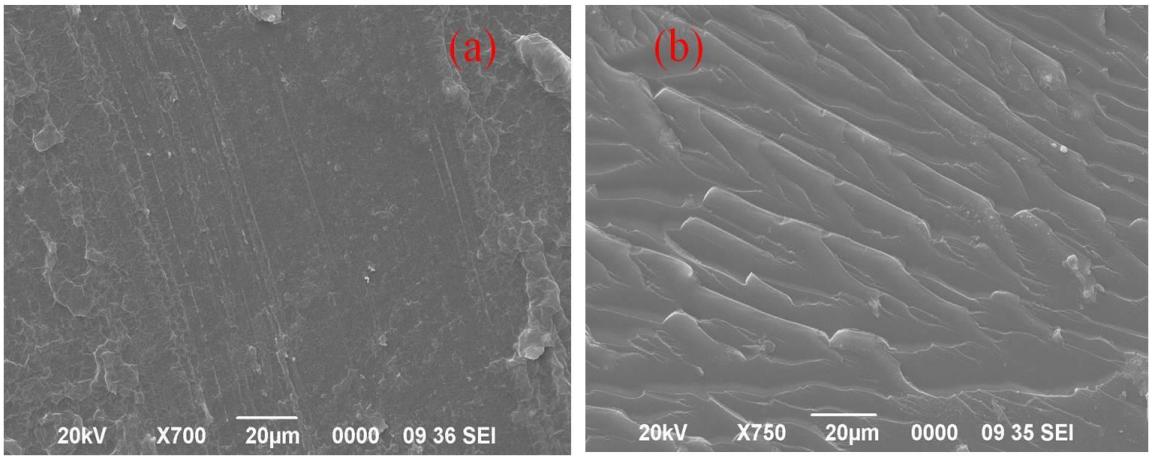

Fig. 3.5: SEM images of (a) HNIPU30 and (b) HNC1.0.

The bulk morphology of the nanocomposite was examined by TEM analysis and the images are shown in **Fig. 3.6**. It is seen that, a uniform dispersion of the AF-GO layers within the polymer matrix has been achieved and not aligned. The TEM micrograph concludes that the GO layers are exfoliated and the polymer chains get intercalated into the layers of GO layers and continue their layered structure in the hybrid nanocomposites. The strong interaction *via* chemical bonding like covalent and hydrogen bonding between amine groups of AF-GO with the carbonate groups of CSFO, epoxy groups of epoxy resin facilitate uniform dispersion and exfoliation of AF-GO in the polymer networks.

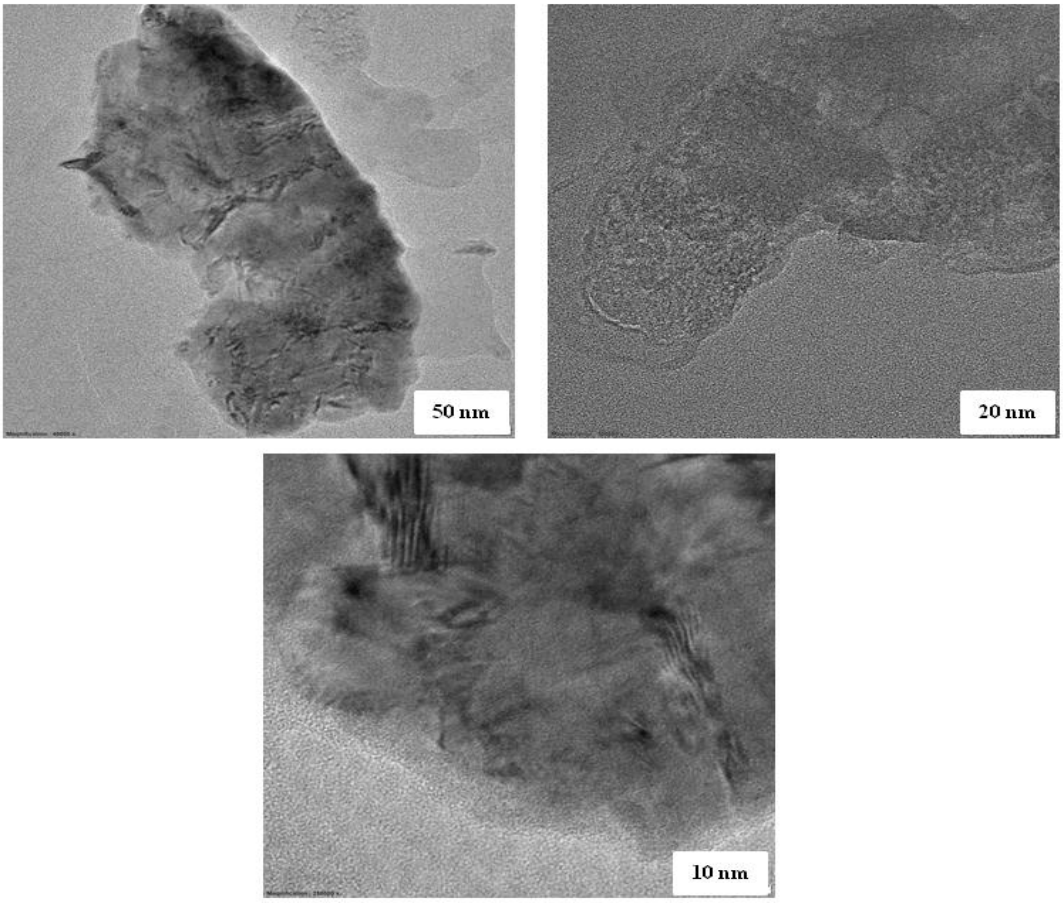

Fig. 3.6: TEM micrographs of the nanocomposites (HNC1.0) at different magnifications.

3.3.4 Mechanical properties

The mechanical properties of HNIPUs and its nanocomposites with different wt% were measured and the results are shown in **Table 3.2**. The influence of epoxy resin in the mechanical properties of HNIPUs was studied by varying its wt% with respect to CSFO. From **Table 3.2**, it is seen that the tensile strength and scratch hardness rise with the increment of epoxy content and incorporation of AF-GO. For example, primarily the tensile strength of the pristine blend (HNIPU30) is 8.4 MPa which increases to 12.5 MPa with the incorporation of 1% AF-GO. The improvement in the properties of the nanocomposites can be ascribed to the high aspect ratio and high strength of graphite platelets and the homogeneous distribution, and also to the hydrogen bonding interactions between hydroxyl H atom and C=O groups present in the polymer matrix, and the strong interaction between the carbonate groups of CSFO, epoxy resin, cyclo-aliphatic IPDA and the amine groups on the surface of AF-GO **(Scheme 3.2)**. Both the

tensile strength and scratch hardness are increased in the nanocomposite in comparison to the HNIPU.

Table 3.2: Performance of the HNIPUs and its nanocomposites.

Sample name	Tensile strength (MPa)	Elongation at break (%)	Scratch hardness (kg)
HNIPU10	5.7	110	4.4
HNIPU20	6.5	98	4.7
HNIPU30	8.4	90	5.5
HNC0.3	9.0	85	5.9
HNC0.6	10.2	75	6.3
HNC1.0	12.5	67	7.0

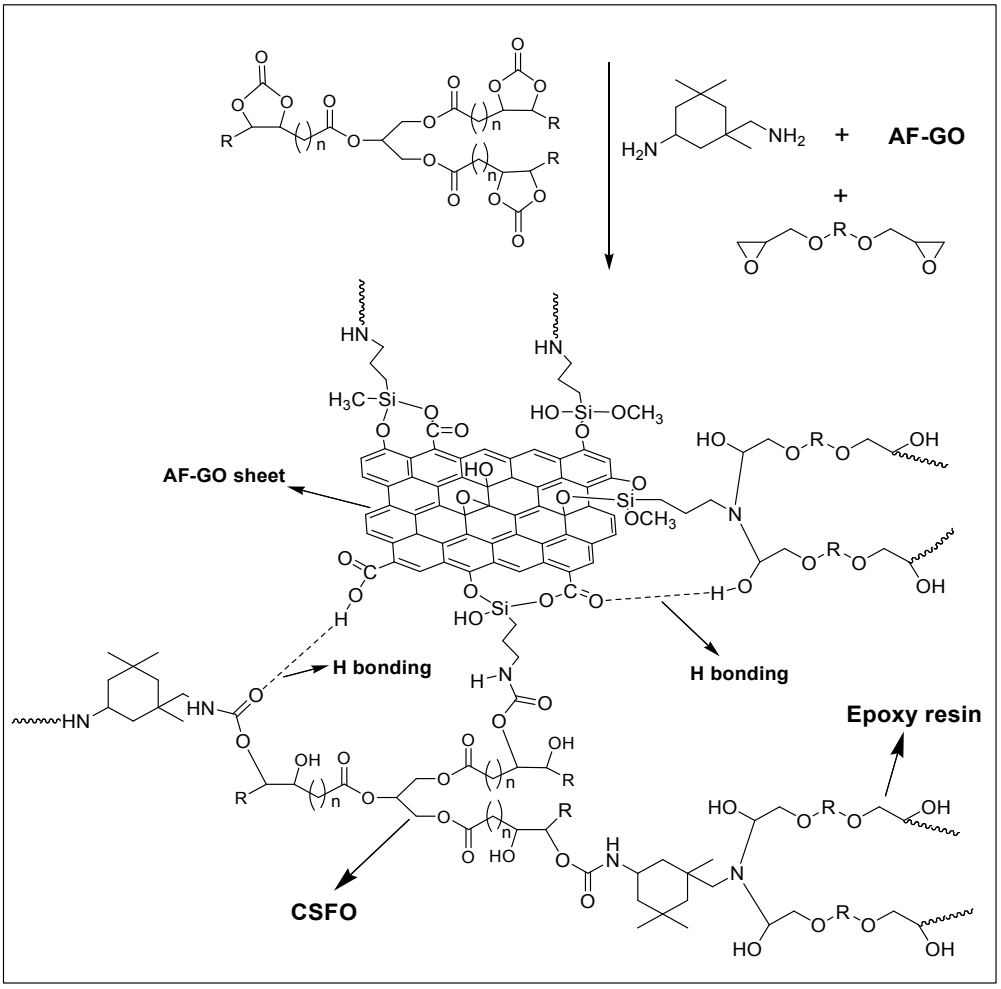

Scheme 3.2: Plausible interactions of AF-GO with the polymer matrix.

3.3.5 Thermal stability

TGA was performed to determine the thermal stability of the nanocomposites as shown in **Fig. 3.7**. From **Table 3.3**, it is observed that the thermal stability of the HNIPU is improved with increasing wt% of AF-GO. For the pristine polymer networks, the initial (5 wt% loss) degradation temperature is found to be 285 °C, whereas for the nanocomposites with 1 wt% (HNC1.0) this value increases to 312 °C. This improvement may be assigned to the strong interfacial interaction between various functional groups present in the constituent like carboxyl, hydroxyl and ester etc. **(Scheme 3.2)**.

Table 3.3: Thermal stability of nanocomposites.

Sample name	Temp @ 5% wt loss (°C)	Temp @ 25% wt loss (°C)	Temp @ 50% wt loss (°C)
HNIPU30	285	353	390
HNC0.3	292	358	400
HNC0.6	301	360	398
HNC1.0	312	363	403

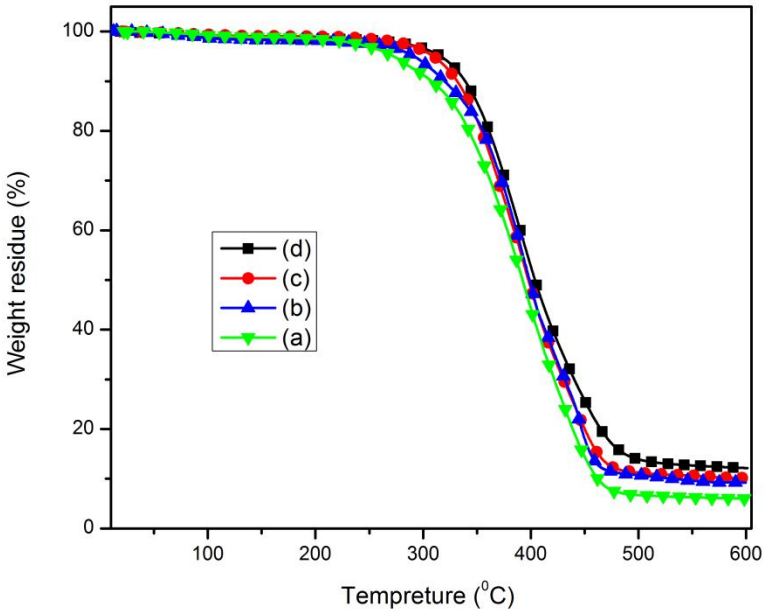

Fig. 3.7: TGA thermograms of HNIPU30, HNC0.3, HNC0.6 and HNC1.0.

3.3.6 Chemical properties

The nanocomposites were tested for their acid, water and alkali resistance by immersion method and the observations are given in **Table 3.4** and the outcomes are listed in **Table 3.4**. The prepared films exhibit excellent resistance to water, ethanol and HCl due to the high cross-linked and good interaction between AF-GO and the HNIPU. But because of the hydrolyzable ester groups, alkali resistance is not satisfactory in pristine HNIPU30. However, due to the chemical interactions of GO sheets in the nanocomposites and cyclic-aliphatic structure of IPDA, the solvent penetration is prevented, and the nanocomposites demonstrate acceptable resistance to alkali.

Table 3.4: Chemical resistance test for the nanocomposite films.

Sample name	Chemical Environment			
	Water	ethanol (25 %, aq.)	NaOH (2%, aq.)	HCl (10%, aq.)
HNIPU30	Excellent	Excellent	Fair	Excellent
HNC0.3	Excellent	Excellent	Good	Excellent
HNC0.6	Excellent	Excellent	Good	Excellent
HNC1.0	Excellent	Excellent	Good	Excellent

Excellent= No weight loss

3.4 Conclusion

In this work, we have developed a series of bio-based NIPU-*blended*-epoxy hybrid materials and its nanocomposites with AF-GO through an environment-friendly and non-isocyanate route. By using different weight wt% of the epoxy resin (10, 20, and 30 wt% with respect to CSFO), a series of HNIPUs were synthesized by using a mixture of CSFO and IPDA. HNIPU with 30 wt% epoxy resin gave the best mechanical properties. Finally, nanocomposites of 30 wt% HNIPU based composition were prepared with AF-GO. As a result, the prepared nanocomposites displayed superior properties than the pristine ones. The hydrogen bonding and covalent interactions of amine functionalized GO with the polymer networks resulted in better performance

characteristics of the nanocomposites. Overall, it can be concluded that the prepared hybrid nanocomposites exhibited a good balance of mechanical, chemical and thermal properties.

3.5 References

[1] Benyahya, S., Habas, J. P., Auvergne, R., Lapinte, V., and Caillol, S. Structure-property relationships in polyhydroxyurethanes produced from terephthaloyl dicyclocarbonate with various polyamines. *Polymer International*, 61(11):1666-1674, 2012.

[2] Yang, J. C., Zhao, C., Hsieh, I. F., Subramanian, S., Liu, L., Cheng, G., Li, L., Cheng, S. Z. D., and Zheng, J. Strong resistance of poly (ethylene glycol) based L-tyrosine polyurethanes to protein adsorption and cell adhesion. *Polymer International*, 61(4):616-621, 2012.

[3] Poussard, L., Lazko, J., Mariage, J., Raquez, J. M., and Dubois, P. Biobased waterborne polyurethanes for coating applications: How fully biobased polyols may improve the coating properties. *Progress in Organic Coatings*, 97:175-183, 2016.

[4] Levchik, S. V and Weil, E. D. Thermal decomposition, combustion and fire-retardancy of polyurethanes-a review of the recent literature. *Polymer International*, 53(11):1585-1610, 2004.

[5] Król, P. Synthesis methods, chemical structures and phase structures of linear polyurethanes. Properties and applications of linear polyurethanes in polyurethane elastomers, copolymers and ionomers. *Progress in Materials Science*, 52(6):915-1015, 2007.

[6] Anderson, J. M., Hiltner, A., Wiggins, M. J., Schubert, M. A., Collier, T. O., Kao, W. J., and Mathur, A. B. Recent advances in biomedical polyurethane biostability and biodegradation. *Polymer International*, 46(3):163-171, 1998.

[7] Martina, M. and Hutmacher, D. W. Biodegradable polymers applied in tissue engineering research: a review. *Polymer International*, 56(2):145-157, 2007.

[8] Deepa, P. and Jayakannan, M. Solvent-free and nonisocyanate melt transurethane reaction for aliphatic polyurethanes and mechanistic aspects. *Journal of Polymer Science Part A: Polymer Chemistry*, 46(7):2445-2458, 2008.

[9] Palaskar, D. V., Boyer, A., Cloutet, E., Alfos, C., and Cramail, H. Synthesis of biobased polyurethane from oleic and ricinoleic acids as the renewable resources via the AB-type self-condensation approach. *Biomacromolecules*, 11(5):1202-1211, 2010.

[10] Tomita, H., Sanda, F., and Endo, T. Reactivity comparison of five- and six-membered cyclic carbonates with amines: Basic evaluation for synthesis of poly(hydroxyurethane). *Journal of Polymer Science Part A: Polymer Chemistry*, 39(1):162-168, 2001.

[11] Xu, S., Li, C., Li, H., Li, M., Qu, C., and Yang, B. Carbon dioxide sensors based on a surface acoustic wave device with a graphene-nickel-l -alanine multilayer film. *Journal of Materials Chemistry C*, 3(16):3882-3890, 2015.

[12] Yang, Z. Z., He, L. N., Gao, J., Liu, A. H., and Yu, B. Carbon dioxide utilization with C–N bond formation: Carbon dioxide capture and subsequent conversion. *Energy & Environmental Science*, 5(5):6602, 2012.

[13] Rokicki, G., Parzuchowski, P. G., and Mazurek, M. Non-isocyanate polyurethanes: Synthesis, properties, and applications. *Polymers for Advanced Technologies*, 26(7):707-761, 2015.

[14] Jalilian, M., Yeganeh, H., and Haghighi, M. N. Synthesis and properties of polyurethane networks derived from new soybean oil-based polyol and a bulky blocked polyisocyanate. *Polymer International*, 57(12):1385-1394, 2008.

[15] Bähr, M., Bitto, A., and Mülhaupt, R. Cyclic limonene dicarbonate as a new monomer for non-isocyanate oligo- and polyurethanes (NIPU) based upon terpenes. *Green Chemistry*, 14(5):1447, 2012.

[16] Javni, I., Hong, D. P., and Petrović, Z. S. Soy-based polyurethanes by nonisocyanate route. *Journal of Applied Polymer Science*, 108(6):3867-3875, 2008.

[17] Tamami, B., Sohn, S., and Wilkes, G. L. Incorporation of carbon dioxide into soybean oil and subsequent preparation and studies of nonisocyanate polyurethane networks. *Journal of Applied Polymer Science*, 92(2):883-891, 2004.

[18] Doll, K. M. and Erhan, S. Z. The improved synthesis of carbonated soybean oil using supercritical carbon dioxide at a reduced reaction time. *Green Chemistry*, 7(12):849, 2005.

[19] Rokicki, G. and Piotrowska, A. A new route to polyurethanes from ethylene carbonate, diamines and diols. *Polymer*, 43(10):2927-2935, 2002.

[20] Kihara, N. and Endo, T. Synthesis and properties of poly(hydroxyurethane)s. *Journal of Polymer Science Part A: Polymer Chemistry*, 31(11):2765-2773, 1993.

[21] Doley, S. and Dolui, S. K. Solvent and catalyst-free synthesis of sunflower oil based polyurethane through non-isocyanate route and its coatings properties. *European Polymer Journal*, 102:161-168, 2018.

[22] Gogoi, P., Boruah, M., Sharma, S., and Dolui, S. K. Blends of epoxidized alkyd resins based on jatropha oil and the epoxidized oil cured with aqueous citric acid solution: A Green technology approach. *ACS Sustainable Chemistry & Engineering*, 3(2):261-268, 2015.

[23] Tomita, H., Sanda, F., and Endo, T. Structural analysis of polyhydroxyurethane obtained by polyaddition of bifunctional five-membered cyclic carbonate and diamine based on the model reaction. *Journal of Polymer Science Part A: Polymer Chemistry*, 39(6):851-859, 2001.

[24] Burgel, T. and Fedtke, M. Reactions of cyclic carbonates with amines: Model studies for curing process. *Polymer Bulletin*, 27(2):171-177, 1991.

[25] Besse, V., Camara, F., Méchin, F., Fleury, E., Caillol, S., Pascault, J. P., and Boutevin, B. How to explain low molar masses in polyhydroxyurethanes (PHUs). *European Polymer Journal*, 71:1-11, 2015.

[26] Tomita, H., Sanda, F., and Endo, T. Polyaddition behavior of bis(five- and six-membered cyclic carbonate)s with diamine. *Journal of Polymer Science Part A: Polymer Chemistry*, 39(6):860-867, 2001.

[27] Tomita, H., Sanda, F., and Endo, T. Polyaddition of bis(seven-membered cyclic carbonate) with diamines: A novel and efficient synthetic method for polyhydroxyurethanes. *Journal of Polymer Science Part A: Polymer Chemistry*, 39(23):4091-4100, 2001.

[28] Tang, D., Mulder, D.-J., Noordover, B. A. J., and Koning, C. E. Well-defined Biobased Segmented Polyureas Synthesis via a TBD-catalyzed Isocyanate-free Route. *Macromolecular Rapid Communications*, 32(17):1379-1385, 2011.

[29] Ke, J., Li, X., Wang, F., Kang, M., Feng, Y., Zhao, Y., and Wang, J. The hybrid polyhydroxyurethane materials synthesized by a prepolymerization method from CO2-sourced monomer and epoxy. *Journal of CO_2 Utilization*, 16:474-485, 2016.

[30] Figovsky, O., Shapovalov, L., and Axenov, O. Advanced coatings based upon non-isocyanate polyurethanes for industrial applications. *Surface Coatings International Part B: Coatings Transactions*, 87(2):83-90, 2004.

[31] Wazarkar, K., Kathalewar, M., and Sabnis, A. Development of epoxy-urethane hybrid coatings via non-isocyanate route. *European Polymer Journal*, 84:812-827, 2016.

[32] Lee, C. Y., Bae, J. H., Kim, T. Y., Chang, S. H., and Kim, S. Y. Using silane-functionalized graphene oxides for enhancing the interfacial bonding strength of carbon/epoxy composites. *Composites Part A: Applied Science and Manufacturing*, 75:11-17, 2015.

[33] Lee, S., Hong, J.-Y., and Jang, J. The effect of graphene nanofiller on the crystallization behavior and mechanical properties of poly(vinyl alcohol). *Polymer International*, 62(6):901-908, 2013.

[34] Wu, F., Lu, Y., Shao, G., Zeng, F., and Wu, Q. Preparation of polyacrylonitrile/graphene oxide by in situ polymerization. *Polymer International*, 61(9):1394-1399, 2012.

[35] Wang, J., Wang, X., Xu, C., Zhang, M., and Shang, X. Preparation of graphene/poly(vinyl alcohol) nanocomposites with enhanced mechanical properties and water resistance. *Polymer International*, 60(5):816-822, 2011.

[36] Jiang, T., Kuila, T., Kim, N. H., Ku, B. C., and Lee, J. H. Enhanced mechanical properties of silanized silica nanoparticle attached graphene oxide/epoxy composites. *Composites Science and Technology*, 79:115-125, 2013.

[37] Pourhashem, S., Rashidi, A., Vaezi, M. R., and Bagherzadeh, M. R. Excellent corrosion protection performance of epoxy composite coatings filled with amino-silane functionalized graphene oxide. *Surface and Coatings Technology*, 317:1-9, 2017.

[38] Nikafshar, S., Zabihi, O., Hamidi, S., Moradi, Y., Barzegar, S., Ahmadi, M., and Naebe, M. A renewable bio-based epoxy resin with improved mechanical performance that can compete with DGEBA. *RSC Advances*, 7(14):8694-8701, 2017.

[39] Ma, W., Wu, L., Zhang, D., and Wang, S. Preparation and properties of 3-aminopropyltriethoxysilane functionalized graphene/polyurethane nanocomposite coatings. *Colloid and Polymer Science*, 291(12):2765-2773, 2013.